Hindawi Publishing Corporation
Journal of Chemistry
Volume 2014, Article ID 940579, 10 pages
http://dx.doi.org/10.1155/2014/940579

Research Article

Effect of the Diesel, Inhibitor, and CO_2 Additions on the Corrosion Performance of 1018 Carbon Steel in 3% NaCl Solution

J. Porcayo-Calderon,[1,2] M. Casales-Diaz,[2] L. M. Rivera-Grau,[1] D. M. Ortega-Toledo,[2] J. A. Ascencio-Gutierrez,[2] and L. Martinez-Gomez[2,3]

[1] *Universidad Autonoma del Estado de Morelos, CIICAp, Avenida Universidad 1001, 62209 Cuernavaca, MOR, Mexico*
[2] *Universidad Nacional Autonoma de Mexico, Instituto de Ciencias Fisicas, Avenida Universidad s/n, 62210 Cuernavaca, MOR, Mexico*
[3] *Corrosion y Proteccion, Buffon 46, 11590 Mexico City, DF, Mexico*

Correspondence should be addressed to J. Porcayo-Calderon; jporcayoc@gmail.com

Received 26 May 2014; Revised 2 August 2014; Accepted 4 August 2014; Published 19 August 2014

Academic Editor: Stojan Stavber

In order to determine the diesel contribution in the coadsorption process of the oil-soluble inhibitors, electrochemical impedance spectroscopy measurements have been carried out to study the performance of oil-soluble inhibitors in both presence and absence of diesel and CO_2. The results showed that the presence of the oil phase provides some protection to the steel because the water-soluble fractions are capable of being adsorbed on the steel surface thereby reducing the corrosion rate. The oily phase does not contribute to the adsorption process of the inhibitor because the inhibitor is absorbed into the water-soluble fractions. The oil-soluble inhibitors are effective only when the solution is saturated with CO_2. CO_2 saturation causes a decrease in the pH of the solution causing both an increase of the inhibitor solubility and a better dispersion of the inhibitor into the electrolyte.

1. Introduction

Because of its importance in several industrial processes, the corrosion of carbon steel in CO_2-containing solutions is a well-known problem that has been investigated for many years. One of these industrial processes is oil and gas production and transport. In the oil industry, it is common to find hydrocarbons containing carbon dioxide (CO_2). Further, the presence of water, CO_2, and impurities, such as chlorides, promotes the corrosion phenomenon. CO_2 can be dissolved in aqueous environments generating highly corrosive solutions. Corrosion under these conditions occurs generally in oxygen-free environment. During this corrosion process, the carbon steel surface can be covered by a corrosion scale ($FeCO_3$), which could slow down the corrosion rate and could protect the substrate from further corrosion. However the type of CO_2 corrosion varies according to the precise environmental conditions, such that an increment of the temperature, pressure, or flow conditions could also increase the aggressiveness of these fluids on iron and low alloy steels [1, 2].

The problems arising from CO_2 corrosion have led to the development of various methods of corrosion control which include the injection of corrosion inhibitors that has proven to be a practical and economical method to control CO_2 corrosion. Nitrogen-based organic surfactants, such as imidazoline and its derivatives, have been used successfully as inhibitors in combating CO_2 corrosion. These organic compounds inhibit the corrosion of mild steel by adsorption on the metal-solution interface thereby creating a barrier that prevents the active ions in the corrosion reactions from getting to the surface [3, 4].

It has been demonstrated that aqueous CO_2 corrosion of carbon steel is an electrochemical process involving the anodic dissolution of iron and the cathodic evolution of hydrogen [4]. This protection process is due to the hydration of CO_2 to give carbonic acid as follows:

$$CO_2 + H_2O \longrightarrow H_2CO_3 \quad (1)$$

Since the solution is deaerated, the dominant cathodic reactions are the reduction of H^+ ions, dissociation of carbonic acid, and water reduction:

$$H_2CO_2 + e^- \longrightarrow H^+ + HCO_3^- \quad (2)$$

$$HCO_3^- + e^- \longrightarrow H^+ + CO_3^{-2} \quad (3)$$

$$2H^+ + 2e^- \longrightarrow H_2 \quad (4)$$

$$2H_2O + 2e^- \longrightarrow 2OH^- + H_2 \quad (5)$$

The main anodic reaction, in absence of oil-soluble inhibitor, is iron dissolution according to

$$Fe \longrightarrow Fe^{+2} + 2e^- \quad (6)$$

During this corrosion process, a corrosion scale of iron carbonate, $FeCO_3$, would form onto steel surface according to

$$Fe^{+2} + CO_3^{-2} \longrightarrow FeCO_3 \quad (7)$$

The steel corroded in the uninhibited solution shows porous corrosion products with some cracks, where the electrolyte can penetrate and corrode the steel surface detaching the corrosion products layer [2]. On the other hand, the corrosion rate reduction of the steel exposed into inhibited solutions is due to the inhibitor film adhered onto the steel surface which improves the growth of a corrosion products layer more compact, forming an effective barrier against the ingress of the aggressive environment. Studies report that the adsorption of the organic inhibitors mainly depends on some physicochemical properties of the molecule, related to its functional groups, to the possible steric effects, and to electronic density of donor atoms. Adsorption is supposed to depend on the possible interaction of the π-orbitals of the inhibitor with the d-orbitals of the surface atoms, which induce greater adsorption of the inhibitor molecules onto the surface of metal, leading to the formation of a corrosion protection film [5].

However, in the case of oil-soluble inhibitors, it is important to know the effect of the electrolyte components on the transport of the inhibitor to the steel surface where the absorption process takes place. It has been reported that the inhibitor would be transported to the surface when the oily part was present. Thus, it seems that the presence of the oily phase has an effect of coadsorption of the inhibitor on the substrate, which improved the performance of the inhibitor [6–8].

The purpose of this paper is to evaluate the performance of oil-soluble inhibitors on the corrosion resistance of 1018 carbon steel in both presence and absence of diesel and CO_2 using electrochemical technique. This can determine the diesel contribution to the coadsorption process of the oil-soluble inhibitors.

2. Experimental

Material tested was a 1018 carbon steel cylinder measuring 25 mm in length and 5.0 mm in diameter. Before testing, the electrode was polished to 600 grit SiC emery paper and then cleaned with alcohol, acetone, and distilled water.

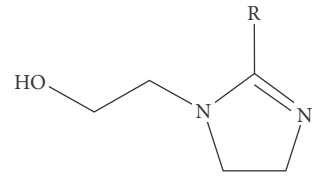

Figure 1: General structure of hydroxyethyl-imidazoline-type inhibitors used, where R is an alkyl chain of 12C for inhibitor A and an oleic chain from coconut oil for inhibitor B.

Inhibitors used in this work include a commercial hydroxyethyl-imidazoline (inhibitor A) and an imidazoline (inhibitor B) which resulted from modifying inhibitor A with coconut oil. The synthesis of coconut oil based inhibitor is detailed elsewhere [9]. In general, imidazoline compounds present a pendant group, an imidazoline head group (a five-member ring containing nitrogen elements), and a hydrocarbon tail, as shown in Figure 1. Molecular modeling studies suggest that the head and pendant group promote bonding of the molecule to the surface, while the hydrocarbon tail forms a protective monolayer. Imidazolines are strongly cationic chemical compounds. The ability of imidazolines to form cations means they are strongly adsorbed onto negatively charged surfaces of metals; thereby these hydrophilic surfaces are converted to hydrophobic surfaces [10]. Hydrophobic head group was an alkyl chain of 12C for inhibitor A and an oleic chain from coconut oil for inhibitor B.

The inhibitors were dissolved in pure 2-propanol. The concentration of the inhibitor used in this work was 25 ppm. Testing solution consisted of 3% NaCl solution at 50°C, and the effect of adding either diesel, inhibitors, or CO_2 and their combinations was studied. Inhibitor was added 2 h after precorroding the specimens in the solution, starting the measurements 1 h later. 3% NaCl solution was deaerated by purging with CO_2 gas during 2 hours prior to the experiment and kept bubbling throughout the experiment.

Electrochemical technique employed was electrochemical impedance spectroscopy (EIS) measurements. Measurements were obtained by using a conventional three-electrode glass cell. A saturated calomel electrode (SCE) was used as the reference electrode with a Luggin capillary bridge, and a high density and high surface area graphite rod was used as the counter electrode. All impedance data were recorded under open-circuit conditions using a sinusoidal excitation voltage of 10 mV and a frequency interval of 0.01–100 KHz. A model PC4 300 Gamry potentiostat was used.

3. Results and Discussion

3.1. Effect of the Addition of Diesel to 3% NaCl Solution. Bode diagrams for carbon steel exposed to 3% NaCl + diesel solution (90 : 10 ratio) at 50°C are shown in Figure 2 (uninhibited solution). In general, three frequency regions referring to the high, intermediate, and low frequency values are observed from Bode diagrams [11]. In the high frequency region it is observed that the $\log|Z|$ values tend to a constant ($\log|Z|$

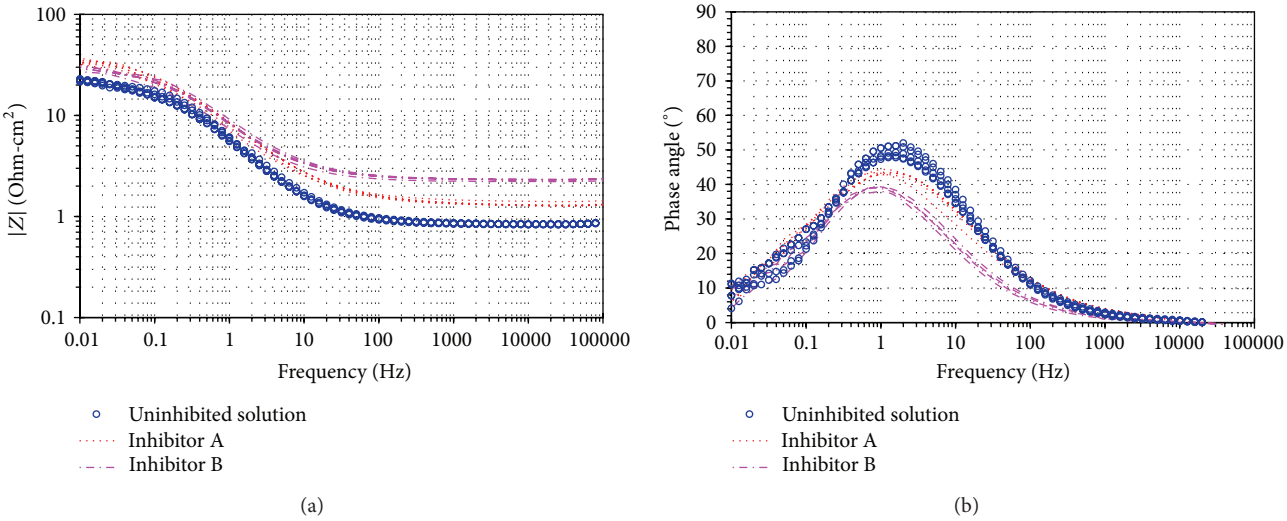

FIGURE 2: Bode plots in the (a) impedance module and (b) phase angle format for carbon steel in the 3% NaCl + diesel solution with and without inhibitors A and B at 50°C.

becomes independent of frequency) where the phase angle approaches zero. The constant value observed corresponds to the solution resistance (R_S).

In the intermediate frequency region, there is a linear relationship between $\log|Z|$ and $\log f$, the slope value is lower than −1, and phase angle value is less than 90°. This indicates that the developed oxide layer has not a capacitive nature and that the corrosion process can be under mixed control (diffusion and charge transfer). The presence of a single phase is observed between 1 and 2 Hz, which is stable as time elapses, and phase angle and the slope of the $\log|Z| - \log f$ relation remain essentially constants. In 3% NaCl solutions the presence of a single phase shift has been observed between 20 and 30 Hz, which is shifting to lower frequencies as time elapses, and this change was associated with a decrease of the phase angle and with a steady decrease in the slope of the $\log|Z| - \log f$ relation [12]. Then it can be considered that the presence of the oil phase provides some protection to the steel surface, possibly due to the formation of a class of oil-water emulsion, and then the oil could diffuse through the aqueous phase until the metal surface to protect it or limit the diffusion of aggressive ions. Another study suggests [13] that the oil phase is capable of being adsorbed on the steel surface thereby reducing the corrosion rate, besides affecting the mass transfer processes to be mix controlled with the charge transfer. On the other hand, it has been reported that the solubility of diesel in water is around 0.5–7 mg/L at room temperature [14], and the water-soluble fractions (WSFs) contain a mixture of C4 to C6 nonaromatic hydrocarbons which are mostly saturated butanes, pentanes, and hexanes and several monoaromatics including benzene, toluene, and xylenes [15]. According to the test conditions, it is possible that the water-soluble fraction is greater, and therefore the solution resistance increased as compared to that observed in the absence of the oily phase [12].

In the low frequency region, it is observed that the $\log|Z|$ values tend to a constant (impedance is independent of the frequency) and the phase angle approximates to zero. The maximum value observed in the plateau region remains virtually constant over time which confirms that the diesel addition provided protection to the steel surface. It is observed that the phase angle trends to zero at frequencies below 0.01 Hz, and a scattering in the experimental data is observed in this region. It is known that in this region are detected the electron charge transfer processes, the mass transfer processes, or other relaxation processes taking place at the film-electrolyte interface or within the pores of the surface film.

3.2. Effect of the Addition of Diesel and Inhibitors to 3% NaCl Solution. From Figure 2 are observed the Bode diagrams for 1018 carbon steel exposed to 3% NaCl + diesel solution plus either inhibitor A or inhibitor B. In both cases it is observed that, in the high frequency range, the $\log|Z|$ values tend to a constant where the phase angle approaches zero. The plateau region begins to form at the same frequency, and the formation of a new phase angle loop is not observed; similar behavior was observed with the uninhibited solution. However, an increase in the solution resistance is shown, being greater with the addition of inhibitor B. It has been reported that in the case of the oil-soluble inhibitors the efficiency may be influenced by the presence of the oily phase, because the presence of the oily phase has an effect of coadsorption of the inhibitor on the substrate to improve the inhibitor performance [6–8]. However, these results show that the presence of the oily phase does not contribute to the adsorption of the inhibitor onto steel surface, and possibly the inhibitor is absorbed by the WSFs. This limits the inhibitor performance and only contributes to increasing the solution resistance.

In the intermediate frequency region, there is a linear relationship between $\log|Z|$ and $\log f$. The values of slopes and phase angles are lower than those observed in the uninhibited solution. This indicates that the corrosion process is

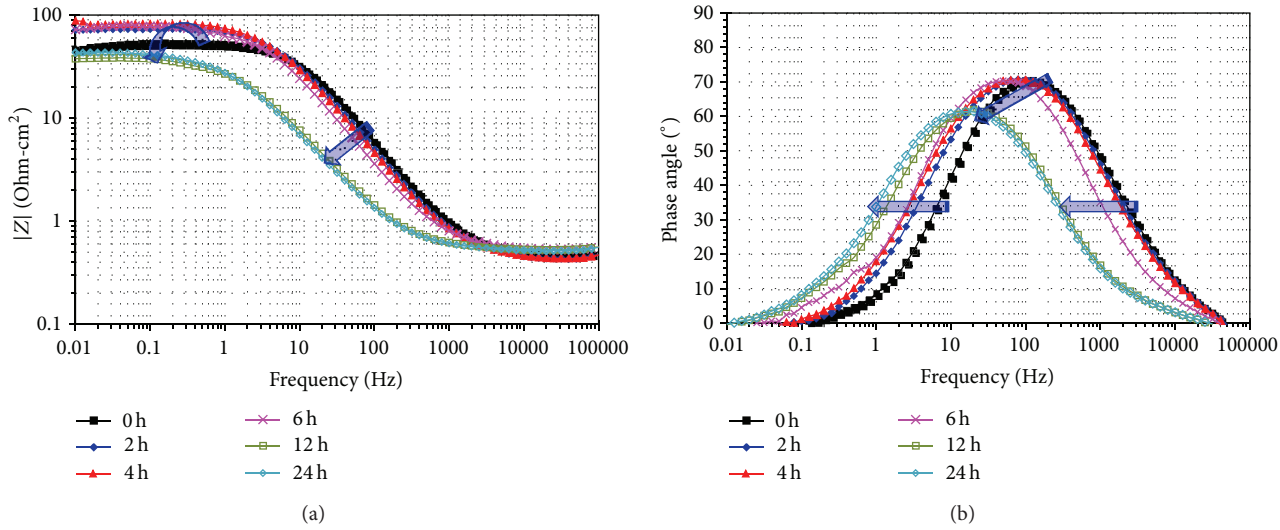

FIGURE 3: Bode plots in the (a) impedance module and (b) phase angle format for carbon steel in the CO_2-saturated (3% NaCl + diesel) solution without inhibitors at 50°C.

being affected by diffusion due to the fact that both phase angles and slopes are close to 45° and −0.5, respectively [16], so the addition of inhibitors favors this phenomenon due to a further increase in the solution resistivity. This effect was more pronounced with the addition of inhibitor B, as it has been noted in the absence of the oily phase [12].

In the low frequency region, in both cases it is observed that the log $|Z|$ values tend to a constant and the phase angle approximates to zero. The maximum values observed in the plateau region show a tendency to increase slightly over time, and these values are greater than those of the uninhibited solution. The increase in impedance module ($|Z|$) can be associated with the increase in the solution resistance due to the absorption of the inhibitors into the WSFs. As it was said, according to the phase angle spectrum there was no evidence of the formation of a protective film of inhibitor on the steel surface in the high frequency region, or is it possible that the adsorption process requires more time to achieve the formation of a film of inhibitor on the steel surface. Studies on CO_2-saturated 3% NaCl solutions showed that imidazoline-base inhibitors provide good protection against corrosion by the formation of a protective film on the steel surface [3, 4, 17, 18]. Then the process of adsorption to the imidazoline-type inhibitors is enhanced by the presence of CO_2 in the electrolyte and not by the oily phase present.

3.3. Effect of the Addition of Diesel and CO_2 to 3% NaCl Solution. Bode diagram for carbon steel exposed to a CO_2-saturated (3% NaCl + diesel) solution at 50°C is shown in Figure 3. In the high frequency region it is observed that the log $|Z|$ values tend to a constant where the phase angle approaches zero. In this case it is observed that the solution resistance is less than that found in 3% NaCl-diesel solution (Figure 1) (uninhibited solution). In previous studies it was found that for 3% NaCl solution the impedance module was less than 0.2 at the high frequency region [12], and according to Figure 1 (uninhibited solution), diesel addition increased the impedance module to 0.9, and in this case with further addition of CO_2 it decreases to 0.5. This may be because the CO_2 dissolved decreases the WSFs or enhances the dispersion of diesel in water. Eliyan and Alfantazi [13] found that, in the carbonated conditions, the addition of oil decreases both the corrosion rates and corrosion potentials and modifies the mass-limit reduction of H^+ and/or H_2CO_3, and the high frequency semicircles are substantially depressed followed by inductive loops resulting from the adsorbed oil layers. Also in the case of 3% NaCl solution, the plateau begins to form at frequencies around 1,000 Hz [12], and with the addition of diesel it begins to form around 100 Hz (Figure 2), and now with the further addition of CO_2 it begins to develop at frequencies around 10,000 Hz (Figure 3). These changes may be associated with the interaction of CO_2 with the electrolyte and the metal surface, which favors the formation of a protective layer onto surface steel.

From the intermediate frequency region, it is observed that the slope value is greater than that observed in the 3% NaCl-diesel solution and similarly the phase angle value (Figure 2). However, the phase angle value after 6 hours decreases and shifts to lower frequencies; the maximum value is observed around 20 Hz. This is consistent with that observed in the low frequency region; in this region as time elapses, the impedance module ($|Z|$) increases but after 6 hours it decreases, increasing thus the corrosion rate. This is evidence of the nonprotective nature of the corrosion products because the CO_2 corrosion of carbon steels is strongly dependent on the surface formed films during the corrosion processes. It is known that the protectiveness, rate of formation/precipitation, and the stability of the film control the corrosion rate and its nature. The main formed film during CO_2 corrosion of carbon steels is iron carbonate, $FeCO_3$, which is affected by iron and carbonate concentrations and temperature. Thus, it seems that $FeCO_3$ film remains on the steel surface for a short time period, and after this time, the corrosion rate increases. This is consistent with

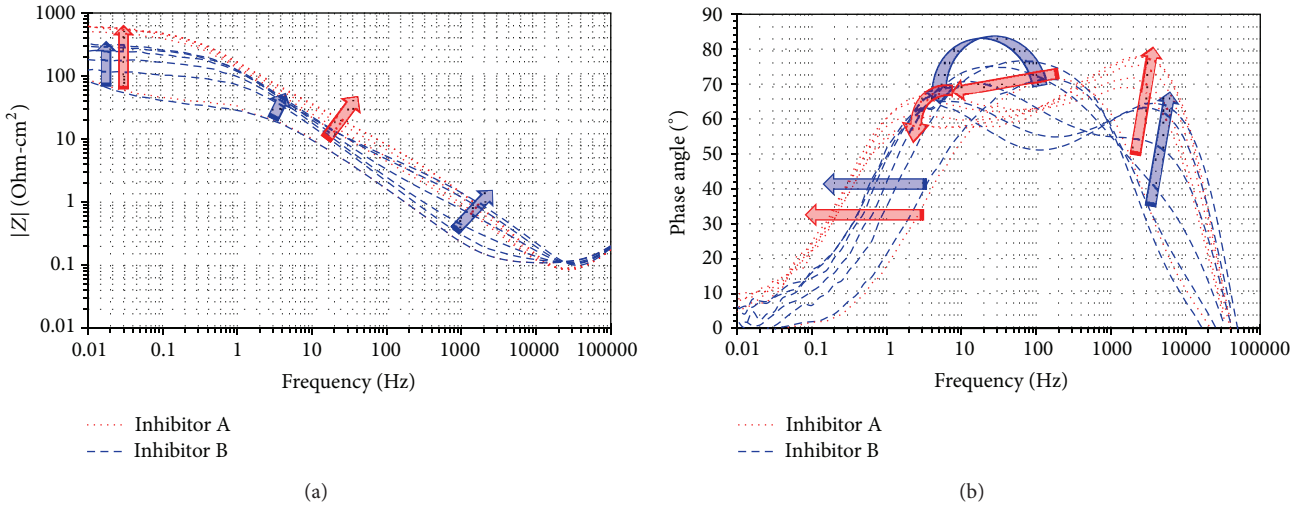

FIGURE 4: Bode plots in the (a) impedance module and (b) phase angle format for carbon steel in the CO_2-saturated (3% NaCl + diesel) solution with inhibitors A and B at 50°C.

the evolution of the phase angle, where there is a maximum in the phase angle (70°) in the first 6 hours but it accompanied with a shift toward low frequency, and after that, the phase angle is reduced at 60°, and this is evidence of a decrease in the capacitive property of the protective films developed on the carbon steel surface. The displacement of the spectrum of phase angle toward lower frequencies may be associated with detachment or thinning of the protective films. These results were consistent with the Nyquist diagram, where it could be observed that the data described a depressed, capacitive-like semicircle, with its center at the real axis, indicating that the corrosion process is under charge transfer control from the metal surface to the solution through the double electrochemical layer, and as time elapsed, the semicircle diameter increased but after 6 hours it decreased. The fact that the semicircle diameter increases and after some time it decreases means that the iron carbonate film increases in thickness reaching a maximum value and after that time either it was detached from the steel surface or it was thinned by some dissolution process.

3.4. Effect of the Addition of Diesel, Inhibitors, and CO_2 to 3% NaCl Solution. From Figure 4 are observed the Bode diagrams for 1018 carbon steel exposed in the CO_2-saturated (3% NaCl + diesel) solution with inhibitors A and B at 50°C. In both cases it is observed that, in the high frequency range, the $\log|Z|$ values tend to a constant where the phase angle approaches zero, and the plateau region begins to form at higher frequencies than 100,000 Hz, with a tendency to those values of the uninhibited solution (Figure 3). In the intermediate frequency region, there is a linear relationship between $\log|Z|$ and $\log f$, and two regions with different slopes are observed. Phase angle-frequency relationship shows the evolution of a new loop at higher frequencies and its value increases over time. The presence of two loops indicates the formation of a protective corrosion products layer. Moreover, a shift to lower frequencies of the intermediate loop is observed. The values of slopes and phase angles are higher than those observed in the uninhibited solution, indicating that the layers formed onto steel surface are more protective than those developed in the uninhibited solution. This effect was more pronounced with the addition of inhibitor A. When both inhibitors are added to the solution, data describe that as time elapses, the impedance module ($|Z|$) increases ten times of magnitude higher than that for uninhibited solution by adding commercial imidazoline (inhibitor A) and almost five times higher by adding the coconut-oil-modified imidazoline (inhibitor B). However, unlike the uninhibited solution, the maximum impedance module ($|Z|$) obtained with both inhibitors reaches a final steady value, indicating the protective nature of the film formed by adding both inhibitors. In the low frequency region, the $\log|Z|$ values tend to a constant and the phase angle approximates to zero. The fact that the $\log|Z|$ values for both imidazolines increase at the beginning and after some time they reach a steady state value indicates the establishment of a protective stable film. As time elapsed, phase angle trends to zero at frequencies below 0.01 Hz, and a scattering in the experimental data is observed. It has been suggested that this type of behavior is because there is a transmissive finite diffusion process and it happens when the thickness of the stagnant layer onto steel surface is finite [19]. This behavior is due to the presence of the inhibitor film onto the steel surface, where the long hydrocarbon chains in the structure of the imidazolines are responsible for their capacity of forming protective barriers against aggressive ions from the bulk solution. In the low frequency region the electron charge transfer processes, the mass transfer processes, or other relaxation processes taking place at the film-electrolyte interface or within the pores of the surface film are detected. The results show that this kind of oil-soluble inhibitors is effective only when the solution is saturated with CO_2. In absence of the oil-soluble inhibitor, corrosion rate reduction has been attributed to the formation of an iron carbonate, $FeCO_3$, film which is affected by iron and carbonate concentrations and temperature. All authors agree that increasing the temperature would improve the

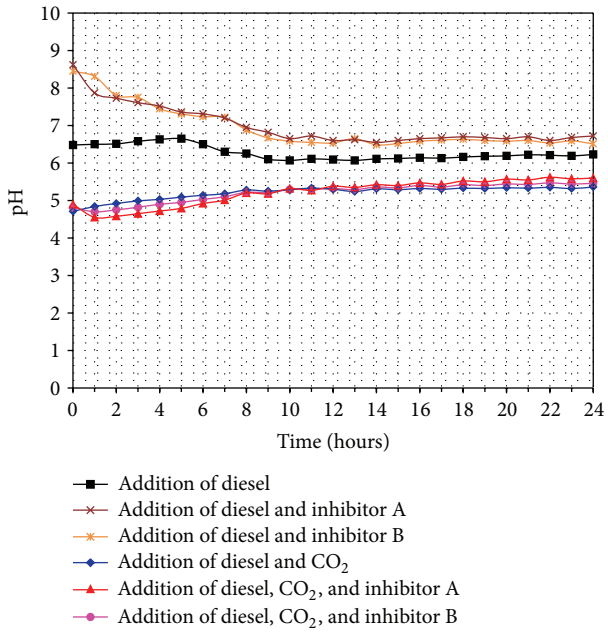

Figure 5: pH value as a function of the time during the corrosion tests.

protectiveness of the $FeCO_3$ scales as well as their adherence and hardness. The lowest temperature necessary to obtain $FeCO_3$ films that would reduce the corrosion rate is 50°C.

Figure 5 shows the pH change as function of the time during the corrosion tests. In general for all test conditions, it can be seen that, during the first 8–10 hours, the pH values show slight fluctuations and then remain practically stable. In the base mixture (diesel-3% NaCl solution), the average pH values were 6.5 for the first 5 hours and then dropped to 6.2 during the remainder of the corrosion test. However, with the addition of inhibitors to the base mixture, the initial pH is 8.5 and then drops to values of 6.7 as time elapsed. This increase in the pH of the base mixture can be understood considering that the imidazoline derivatives are strong bases and quite polar [20]; subsequent decrease in the pH values can be associated with the absorption of the inhibitors into the WSFs; as it was said, there was no evidence of the formation of a protective film of inhibitor on the steel surface. On the other hand, when CO_2 is added to the base mixture, the initial pH is 4.8 and then increases during the first 8 hours until a pH value of 5.3 and thereafter remains constant until the end of the test. When CO_2 is added to the brine, hydrogen ion (H^+) will be in equilibrium with CO_2, and the saturation is achieved in ten minutes and then the pH will be steady [21]. However, the observed decrease in the pH values may be due to the formation of soluble corrosion products, and then increasing the amount of solute in the base mixture, this decreased the CO_2 solubility. It is known that the gas solubility decreases with increasing temperature, increasing salinity, or decreasing pressure. Finally, when both CO_2 and inhibitor are added to the base mixture, the pH values were similar to the trend shown by the base mixture saturated with CO_2. However, pH values were more acidic at the beginning of the test and slightly basic at the end of the test. This can be understood by considering that the imidazolines are amphoteric compounds; that is, they can behave as acids or bases, having similar properties to both pyrrole and pyridine. Imidazoline compounds are susceptible of hydrolysis in aqueous-basic media; however, hydrolysis is not virtually observed at pH < 6, since it needs drastic conditions to decompose the imidazoline structure [22]. Then the process of adsorption to the imidazoline-type inhibitors is enhanced by the reduction in the pH of the solution due to the presence of CO_2 through reactions 1 to 5 causing both an increase of solubility and stability of the inhibitor. Thus the inhibitor can reach the steel surface and not be absorbed onto the WSFs. The difference in the performance of both inhibitors is because coconut oil used for the synthesis of inhibitor B is mainly composed of 12C chains, with appreciable amounts of 10C and 8C chains, and some chains longer than 12C. However, the decreases in the corrosion rate obtained with the modified inhibitor are quite acceptable, which is very encouraging because it provides very promising results in the preparation of green corrosion inhibitors.

3.5. Equivalent Circuits. For the interpretation of the electrochemical behavior of a system from EIS spectra, an appropriate physical model of the electrochemical reactions occurring on the electrodes is necessary. Because the electrochemical cell presents impedance at a small sinusoidal excitation it can be represented by an equivalent circuit. Equivalent circuits are generally used to model the electrochemical behavior and calculate the parameters of interest, such as electrolyte resistance (R_S), charge transfer resistance (R_{ct}), and double layer capacitance (C_{dl}). When a nonideal frequency response is present, it is commonly accepted to employ distributed circuit elements in an equivalent circuit. The most widely used is constant phase element (CPE), which has a noninteger power dependence on the frequency. The impedance of a CPE is described by the expression

$$Z_{CPE} = Y^{-1}(i\omega)^{-n}, \quad (8)$$

where Y is a proportional factor that indicates the combination of properties related to both the surfaces and electroactive species independent of frequency; i is imaginary number ($\sqrt{-1}$); ω is the angular frequency and equal to $2\pi f$, where f is the frequency; and n has the meaning of a phase shift and is related to a slope of the log $|Z|$ versus log frequency plots and usually is in the range 0.5 and 1. When the value of n is equal to 1, the CPE describes an ideal capacitor with Y equal to the capacitance. For $0.5 < n < 1$ the CPE describes a distribution of dielectric relaxation times in frequency space, and when n is equal to 0.5 the CPE represents a Warburg impedance with diffusional character. In these situations the semicircle in the Zre-Zim spectra is more and more depressed. Often, a CPE is used in a model in place of a capacitor to compensate for nonhomogeneity in the system to take into account irregularities of the surface such as roughness or because properties such as double layer capacitance, charge transfer rate are nonuniformly distributed.

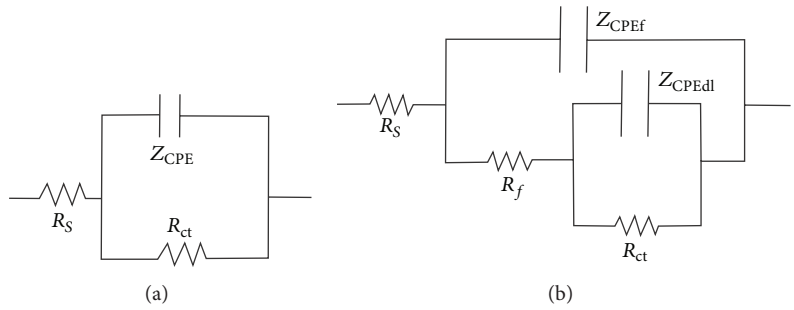

Figure 6: Equivalent circuits used to represent the impedance results: (a) base mixture, inhibitor A in base mixture, inhibitor B in base mixture, and CO_2 in base mixture; (b) CO_2 and inhibitor A in base mixture, CO_2 and inhibitor B in base mixture.

Table 1: Equivalent circuit parameters for base mixture.

Time (min)	R_S (Ω)	R_{ct} (Ω)	Y_{dl} (Ω^{-1} s^n)	n
0	0.837	22.62	0.043597	0.71
3	0.839	22.49	0.0481	0.72
6	0.832	22.41	0.047056	0.72
12	0.842	20.99	0.041319	0.75
18	0.840	21.50	0.03955	0.76
24	0.838	21.81	0.037752	0.78

Table 2: Equivalent circuit parameters for effect of the addition of inhibitor A to base mixture.

Time (min)	R_S (Ω)	R_{ct} (Ω)	Y_{dl} (Ω^{-1} s^n)	n
0	1.42	37.57	0.032962	0.684
3	1.28	36	0.39607	0.656
6	1.29	36.34	0.035179	0.658
12	1.29	37.88	0.035887	0.652
18	1.31	40.34	0.035432	0.656
24	1.32	35.86	0.043927	0.643

Table 3: Equivalent circuit parameters for effect of the addition of inhibitor B to base mixture.

Time (min)	R_S (Ω)	R_{ct} (Ω)	Y_{dl} (Ω^{-1} s^n)	n
0	2.22	26.91	0.043261	0.690
3	2.31	30.14	0.037849	0.688
6	2.32	30.20	0.036078	0.694
12	2.33	29.52	0.035971	0.686
18	2.33	29.31	0.335678	0.691
24	2.34	28.56	0.030777	0.703

Table 4: Equivalent circuit parameters for effect of the addition of CO_2 to base mixture.

Time (min)	R_S (Ω)	R_{ct} (Ω)	Y_{dl} (Ω^{-1} s^n)	n
0	0.474	51.81	0.0005554	0.888
3	0.440	72.98	0.0007500	0.871
6	0.441	82.6	0.0008450	0.826
12	0.539	75.43	0.0010327	0.871
18	0.533	57.73	0.0043739	0.815
24	0.525	42.81	0.0050317	0.807

From the impedance spectra for each analyzed experimental condition, the experimental data can be modeled by the electric equivalent circuits given in Figure 6. For metal electrodes corroded in the presence of diesel, diesel plus inhibitors, and diesel plus CO_2, only one peak is in the phase angle versus frequency plot, indicating that there is only one time constant (Figures 2 and 3). In these cases, the time constant is related to the corrosion process at the metal/corrosion products/electrolyte interphase and can be modelled by a simple Randles equivalent circuit (Figure 6(a)) that allows electrolyte resistance (R_S), charge transfer resistance (R_{ct}), and double layer capacitance calculation (Z_{CPE}). However, for metal electrodes with the inhibitor film adsorbed onto their surface, from phase angle versus frequency plot, two separate peaks can be clearly seen indicating the existence of two time constants (Figure 4). The high frequency time constant indicates the presence of an inhibitor film covering the surface, and the low frequency one is related to corrosion process at the unprotected sites of the metal surface. In this case, the time constants can be modelled by the equivalent circuit shown in Figure 6(b). The equivalent electrical circuit represents a porous inhibitor film formed onto the metal surface, in which Z_{CPEf} is related to the nonideal capacitance of the inhibitor film, R_f to the inhibitor film resistance, which reflects the protective properties of the inhibitor film, and Z_{CPEdl} to the nonideal capacitance of the double layer of the electrolyte/corrosion products/metal interphase. In this case, $R_f < R_{ct}$; hence $Y = Y_f + Y_{dl} \sim Y_{dl}$ [7, 23]. The fitting parameters obtained using the electrical circuit shown in Figure 6 for each analyzed experimental condition are presented in Tables 1, 2, 3, 4, 5, and 6.

Figure 7 shows the variation of R_{ct} for each simulated condition. It can be seen that 1018 carbon steel showed the lowest corrosion resistance in the base mixture. However, its values remain constant over time which confirms that the diesel addition provided protection to the steel surface. Possibly the WSFs either were adsorbed on the steel surface or increased the solution resistance affecting the mass transfer processes. Addition of the inhibitors to the base mixture only caused a light increase in the corrosion resistance of the carbon steel. This can indicate that the oily phase does not contribute to the adsorption of the inhibitor onto steel

Table 5: Equivalent circuit parameters for effect of the addition of CO_2 and inhibitor A to base mixture.

Time (min)	R_S (Ω)	CPE$_f$			R_{ct} (Ω)	CPE$_{dl}$	
		R_f (Ω)	Y_f (Ω^{-1} s^n) $*$ 10^{-5}	n		Y_{dl} (Ω^{-1} s^n) $*$ 10^{-3}	n
0	0.102	—	—	—	32.6	2.42	0.87
3	0.086	3.65	20.873	0.98	506.4	1.38	0.77
6	0.085	4.32	16.495	0.99	621.4	1.38	0.75
12	0.088	3.50	5.984	1.00	676.3	1.52	0.71
18	0.086	5.00	6.070	1.00	677.9	1.44	0.69
24	0.076	7.58	9.988	1.00	621.2	1.28	0.71

Table 6: Equivalent circuit parameters for effect of the addition of CO_2 and inhibitor B to base mixture.

Time (min)	R_S (Ω)	CPE$_f$			R_{ct} (Ω)	CPE$_{dl}$	
		R_f (Ω)	Y_f (Ω^{-1} s^n) $*$ 10^{-5}	n		Y_{dl} (Ω^{-1} s^n) $*$ 10^{-3}	n
0	0.102	—	—	—	33.05	2.43	0.87
3	0.119	0.19	18.02	1.00	112.8	1.69	0.80
6	0.114	0.35	18.16	1.00	175.4	1.36	0.83
12	0.099	1.60	38.26	0.90	243.0	1.07	0.82
18	0.099	2.79	15.37	0.96	313.6	1.46	0.77
24	0.0855	4.60	22.10	0.91	287.3	1.41	0.79

surface; therefore, the addition of inhibitors only contributes to increasing the solution resistivity. On the other hand, the presence of CO_2 dissolved in the base mixture causes an increase in the corrosion resistance of the carbon steel; however the R_{ct} values tend to decrease as time elapses. Clearly the corrosion product layer was not protective. It seems that $FeCO_3$ film increased in thickness reaching a maximum value and after it was detached from the steel surface or it was thinned by some dissolution process. However, when CO_2 dissolved and inhibitors are present in the base mixture, it can be seen that the corrosion resistance of the carbon steel is increased until two orders of magnitude. The fact that the R_{ct} values increase at the beginning and after some time they reach a steady state value indicates the establishment of a protective stable film. This indicates that the layers formed onto carbon steel surface are more protective than those formed in the other solutions. Nevertheless R_f values are low; the values of n indicate the high capacitance of the film inhibitor which limits the charge transfer processes and then increases the corrosion resistance of the carbon steel. Once again, these results show that the oil-soluble inhibitors are effective only when the base mixture is saturated with CO_2.

The surface morphologies of the 1018 carbon steel specimen after the corrosion tests were examined using SEM. In Figure 8 are shown the superficial aspects of the specimens evaluated in the base mixture and in the base mixture with CO_2 and inhibitor A. The surface morphologies of the specimens evaluated in the base mixture with inhibitors, base mixture with CO_2, and base mixture with inhibitors were similar to that of specimen evaluated in the base mixture (Figure 8(a)), and the surface morphology of the specimen evaluated in base mixture with CO_2 and inhibitor B was similar to that of Figure 8(b). It is clear that, in the absence of a protective film stable, the steel surface shows a rough appearance due to a rapid corrosion attack. The attack was

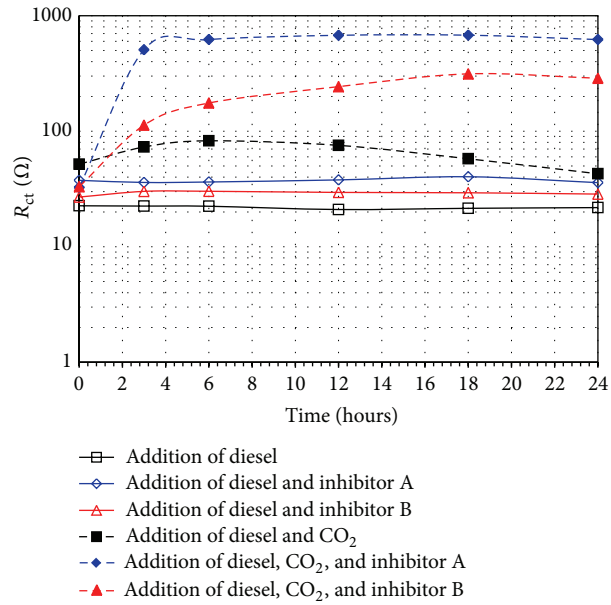

Figure 7: R_{ct} variation for each simulated experimental condition.

general with evidence of localized corrosion. However when the inhibitor is able to be adsorbed onto the steel surface and is forming a protective layer, the surface morphology is visibly less rough and the presence of localized corrosion was not detected, but this was only possible when the inhibitor was added to the CO_2-saturated base mixture.

4. Conclusions

Electrochemical impedance spectroscopy (EIS) measurements have been carried out to study the performance of oil-soluble inhibitors on the corrosion resistance of 1018 carbon

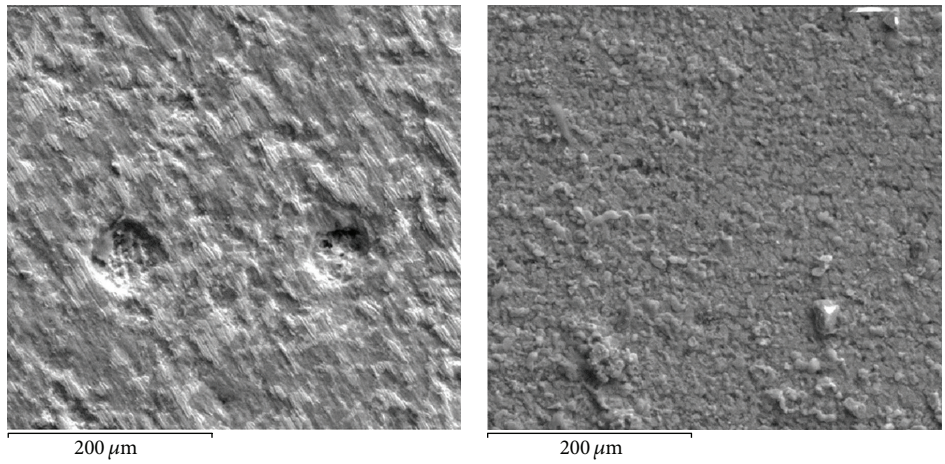

Figure 8: Surface morphology for 1018 carbon steel after the corrosion test: (a) in the base mixture, (b) in the base mixture with CO_2 and inhibitor A.

steel in both presence and absence of diesel and CO_2. The inhibitors under study included a commercial hydroxyethyl-imidazoline (12C) and an imidazoline which resulted from modifying the first one with coconut oil. It was found that the presence of the oil phase provides some protection to the steel, possibly due to the formation of a class of oil-water emulsion, and the WSFs are capable of being adsorbed on the steel surface thereby reducing the corrosion rate, besides affecting the mass transfer processes. The presence of the oily phase does not contribute to the adsorption of the inhibitor onto steel surface, possibly because the inhibitor is absorbed by the WSFs. The oil-soluble inhibitors are effective only when the solution is saturated with CO_2. The formation of the inhibitor film onto the steel surface is caused by a reduction in the pH of the solution due to the presence of CO_2 causing an increase of the inhibitor solubility.

Conflict of Interests

The authors declare that there is no conflict of interests regarding the publication of this paper.

Acknowledgment

Financial support from Consejo Nacional de Ciencia y Tecnología (CONACYT, México) (Project 198687—"Desarrollo de metodologías para la extracción de productos oleicos de coco para su conversión en inhibidores de corrosión orgánicos. Cuarta etapa: escalamiento y transferencia tecnológica") is gratefully acknowledged.

References

[1] S. Arzola, J. Mendoza-Flores, R. Duran-Romero, and J. Genesca, "Electrochemical behavior of API X70 steel in hydrogen sulfide-containing solutions," *Corrosion*, vol. 62, no. 5, pp. 433–443, 2006.

[2] S. L. Wu, Z. D. Cui, F. He, Z. Q. Bai, S. L. Zhu, and X. J. Yang, "Characterization of the surface film formed from carbon dioxide corrosion on N80 steel," *Materials Letters*, vol. 58, no. 6, pp. 1076–1081, 2004.

[3] X. Liu, P. C. Okafor, and Y. G. Zheng, "The inhibition of CO_2 corrosion of N80 mild steel in single liquid phase and liquid/particle two-phase flow by aminoethyl imidazoline derivatives," *Corrosion Science*, vol. 51, no. 4, pp. 744–751, 2009.

[4] X. Liu, Y. G. Zheng, and P. C. Okafor, "Carbon dioxide corrosion inhibition of N80 carbon steel in single liquid phase and liquid/particle two-phase flow by hydroxyethyl imidazoline derivatives," *Materials and Corrosion*, vol. 60, no. 7, pp. 507–513, 2009.

[5] . Bentiss F, M. Traisnel, and M. Lagrenee, "Effects of the diffusion layer characteristics on the performance of polymer electrolyte fuel cell electrodes," *Journal of Applied Electrochemistry*, vol. 31, pp. 449–454, 2001.

[6] W. Villamizar, M. Casales, L. Martinez, J. G. Chacon-Naca, and J. G. Gonzalez-Rodriguez, "Effect of chemical structure of hydroxyethyl imidazolines inhibitors on the CO_2 corrosion in water-oil mixtures," *Journal of Solid State Electrochemistry*, vol. 12, no. 2, pp. 193–201, 2008.

[7] W. Villamizar, M. Casales, J. G. Gonzalez-Rodriguez, and L. Martinez, "CO_2 corrosion inhibition by hydroxyethyl, aminoethyl, and amidoethyl imidazolines in water-oil mixtures," *Journal of Solid State Electrochemistry*, vol. 11, no. 5, pp. 619–629, 2007.

[8] W. Villamizar, M. Casales, J. G. Gonzales-Rodriguez, and L. Martinez, "An EIS study of the effect of the pedant group in imidazolines as corrosion inhibitors for carbon steel in CO_2 environments," *Materials and Corrosion*, vol. 57, no. 9, pp. 696–704, 2006.

[9] L. M. Rivera-Grau, M. Casales, I. Regla, D. M. Ortega-Toledo, J. G. Gonzalez-Rodriguez, and L. Martinez Gomez, "CO_2 Corrosion inhibition by imidazoline derivatives based on coconut oil," *International Journal of Electrochemical Science*, vol. 7, no. 12, pp. 13044–13057, 2012.

[10] D. Bajpai and V. K. Tyagi, "Review: fatty imidazolines: chemistry, synthesis, properties and their industrial applications," *Journal of Oleo Science*, vol. 55, no. 7, pp. 319–329, 2006.

[11] J. E. G. Gonzalez and J. C. Mirza-Rosca, "Study of the corrosion behavior of titanium and some of its alloys for biomedical and dental implant applications," *Journal of Electroanalytical Chemistry*, vol. 471, pp. 109–115, 1999.

[12] L. M. Rivera-Grau, M. Casales, I. Regla et al., "Effect of organic corrosion inhibitors on the corrosion performance of 1018 carbon steel in 3% NaCl solution," *International Journal of Electrochemical Science*, vol. 8, no. 2, pp. 2491–2503, 2013.

[13] F. F. Eliyan and A. Alfantazi, "Electrochemical investigations on the corrosion behavior and corrosion natural inhibition of API-X100 pipeline steel in acetic acid and chloride-containing CO_2-saturated media," *Journal of Applied Electrochemistry*, vol. 42, no. 4, pp. 233–248, 2012.

[14] M. Campos-Pineda, K. Acuna-Askar, J. A. Martinez-Guel et al., "Time and cost efficient biodegradation of diesel in a continuous-upflow packed bed biofilm reactor and effect of surfactant GAELE," *Journal of Chemical Technology and Biotechnology*, vol. 87, no. 8, pp. 1131–1140, 2012.

[15] H. E. Guard, N. G. James, and R. B. Laughlin Jr., "Characterization of gasolines, diesel fuels & their water soluble fractions," Naval Biosciences Laboratory, Naval Supply Center, Oakland, Calif, USA, Contract no. 2-028-120-0, September 1983.

[16] V. Freger and S. Bason, "Characterization of ion transport in thin films using electrochemical impedance spectroscopy, I: principles and theory," *Journal of Membrane Science*, vol. 302, no. 1-2, pp. 1–9, 2007.

[17] X. Zhang, F. Wang, Y. He, and Y. Du, "Study of the inhibition mechanism of imidazoline amide on CO_2 corrosion of Armco iron," *Corrosion Science*, vol. 43, no. 8, pp. 1417–1431, 2001.

[18] F. Farelas and A. Ramirez, "Carbon dioxide corrosion inhibition of carbon steels through bis-imidazoline and imidazoline compounds studied by EIS," *International Journal of Electrochemical Science*, vol. 5, no. 6, pp. 797–814, 2010.

[19] F. Kuang, D. Zhang, Y. Li, Y. Wan, and B. Hou, "Electrochemical impedance spectroscopy analysis for oxygen reduction reaction in 3.5% NaCl solution," *Journal of Solid State Electrochemistry*, vol. 13, no. 3, pp. 385–390, 2009.

[20] J. A. Mollica, G. R. Padmanabhan, and R. Strusz, "Liquid chromatographic analysis of imidazolines," *Analytical Chemistry*, vol. 45, no. 11, pp. 1859–1864, 1973.

[21] Q. Qu, J. Ma, L. Wang, L. Li, W. Bai, and Z. Ding, "Corrosion behaviour of AZ31B magnesium alloy in NaCl solutions saturated with CO_2," *Corrosion Science*, vol. 53, no. 4, pp. 1186–1193, 2011.

[22] S. O. Bondareva, V. V. Lisitskii, N. I. Yakovtseva, and Y. I. Murinov, "Hydrolysis of 1,2-disubstituted imidazolines in aqueous media," *Russian Chemical Bulletin*, vol. 53, no. 4, pp. 803–807, 2004.

[23] L. D. Paolinelli, T. Pérez, and S. N. Simison, "The effect of pre-corrosion and steel microstructure on inhibitor performance in CO_2 corrosion," *Corrosion Science*, vol. 50, no. 9, pp. 2456–2464, 2008.